

Mixed conductivity and potential fluctuations in semi-insulating GaAs:Cr

B. Pistoulet and G. Hamamdjian

*Laboratoire d'Automatique et de Microélectronique de Montpellier, Université des Sciences et Techniques,
place Eugène Bataillon, 34060 Montpellier Cédex, France*

(Received 24 April 1986; revised manuscript received 24 October 1986)

Extensive investigations have been made on the electrical properties of semi-insulating (si) GaAs. However, most of the measurements were performed under dc conditions, and only very few data on the ac and high-frequency conductivity are available. Moreover data related to the thermopower of this material are practically nonexistent. On the other hand, almost all the theories assume implicitly that the semi-insulating crystal is microscopically homogeneous, i.e., free from potential fluctuations. In the case of chromium-doped si-GaAs showing a bipolar conduction, serious inconsistencies concerning galvanomagnetic data are observed. The most striking of them is the discrepancy between the theoretical and experimental values of the intrinsic carrier density n_i , and the disagreement between the signs of Hall and thermoprobe voltages. In this paper, we proceed to a new examination of the mixed conduction process, and derive complete expressions of the transport coefficients by taking into account the existence of long-range potential fluctuations, which play an essential role in semi-insulating (si) materials. It is shown that dc galvanomagnetic measurements are inadequate for the evaluation of the total carrier densities n, p in the conduction and in the valence bands. These densities can be determined only by measuring the high-frequency conductivity limit σ_∞ and the thermoelectric power S versus temperature. Depending on the relative magnitudes of n and p and of the mobilities μ_n, μ_p , the sign of S can be either positive or negative, while R_H is nearly always negative. Original experimental data on the temperature dependence of dc and high-frequency conductivities σ_{dc} and σ_∞ , and of S , between 300 and 450 K are reported for six Cr-doped si-GaAs samples. These samples are n and p type and have mixed conductivity. The results are discussed on the basis of our model, which allows us to reach a complete and coherent understanding of the observed phenomena. In these samples, mixed conduction is due to the accumulation of packets of electrons in potential wells separated in space from packets of holes accumulated in potential hills. Therefore, models assuming a microscopically constant potential in the sample cannot realistically describe the physical state of the sample. On the contrary, by taking into account the existence of long-range potential fluctuations, all the discrepancies reported in the literature can be removed. Finally, the effect of annealing of an “ n -type” sample is analyzed.

I. INTRODUCTION

For more than twenty years, semi-insulating GaAs has been the subject of a large amount of theoretical and experimental studies. Besides the fundamental interest of transport phenomena in high-resistivity semiconductors, the exceptional attention devoted to this material comes from its increasing importance as a substrate in integrated electronic devices. However, despite extensive investigation, many points remain obscure, and no coherent explanation of the transport phenomena in mixed conductivity regime has yet been achieved. The main inconsistencies reported in the literature are the following.

(i) Generally the dc conductivity σ_{dc} and its activation energy are extending over wide ranges (Look,^{1,2} Kitahara *et al.*,³ and Lin *et al.*⁴) and the Fermi energy calculated from these data is often too small in order to correspond to a mixed conductivity regime.

(ii) The zero-magnetic-field conductivity σ_0 flattens out at relatively low temperature as reported by Look^{1,5} and Inoue and Ohyama;⁶ this behavior is generally attributed to surface conduction, and the data are often simply considered as incorrect.

(iii) The intrinsic carrier density determined experimentally by galvanomagnetic measurements (Gooch *et al.*,⁷ Bube,⁸ and Whelan *et al.*⁹) is larger than the theoretical value deduced from the known band structure of the perfect crystal (Blakemore,¹⁰ Sell and Casey,¹¹ and Panish and Casey¹²). The experimental intrinsic carrier density increases as the resistivity ρ_0 at zero magnetic field decreases, as shown by Look,¹ who considered three possible explanations: influence of surface conduction, other mechanisms than mixed conductivity contributing to the magnetic field dependence of R_H and ρ_0 , and/or possible effects of long-lived traps. Betko and Merinsky^{13,14} found $n_{i\text{ expt}} \simeq 1.5n_{i\text{ theor}}$, and Hrivnak¹⁵ proposed to take into consideration the influence of the anisotropy of the valence band on the Hall factor, and suggested¹⁶ that the high value of $n_{i\text{ expt}}$ can be explained by the narrowing of band gap caused by various defects.

(iv) Samples showing mixed conductivity have generally a negative room temperature Hall coefficient R_H , while the sign of the thermoprobe voltage is positive.

In all the papers, the authors make the implicit assumption that the potential is microscopically constant in the material, though, in their pioneer paper, Cronin and Hais-

ty¹⁷ suggested the possible existence of small n -type regions in p -type samples. Shockley and Bardeen¹⁸ mentioned the effect of varying electrostatic potential which makes the bands move up and down together. The existence of long-range potential fluctuations (PF) in compensated semiconductors was considered by Keldysh and Proshko,¹⁹ Fritzsche,²⁰ and Schklowskii and Efros.²¹ PF result from the nonuniform distribution of ionized centers which, in compensated materials, are not screened by free carriers. Pistoulet *et al.*^{22,23} have shown that PF largely affect dc conductivity, photoconductivity, thermopower, ac conductivity, and their temperature dependences. The analytical expressions of the transport coefficients, derived by these authors in the case of transport in a single band, allowed a very accurate fit of the experimental data in various crystalline and amorphous compensated semiconductors.^{24–26}

The purpose of the present paper is now to analyze transport phenomena in the mixed conductivity regime. In this case, PF of large magnitude introduce new effects, because electrons and holes become separated in space, packets of electrons being located in potential wells, and packets of holes in potential hills. Therefore, the transport properties of the semiconductor are surely very different from those of an homogeneous medium, as we shall show below.

In the presence of PF, the densities n_f, p_f of free electrons and free holes which carry the dc current are usually lower^{22,23} than the total average carrier densities n, p in the bands. Thus the dc conductivity $\sigma_{dc} = q(n_f \mu_n + p_f \mu_p)$ is lower than the very-high-frequency conductivity $\sigma_{\infty} = q(n \mu_n + p \mu_p)$. Generally, the authors are measuring Hall coefficient and dc resistivity versus magnetic field. As shown in Sec. II, these quantities depend only on n_f and p_f , and not directly on the total densities of carriers. Thus, in the absence of other information concerning n and p , the usual interpretation which ignores the effect of PF may lead to quite erroneous conclusions. In particular, the Fermi level position which depends on the total carrier densities n, p and on the magnitude of PF cannot be calculated only from the knowledge of σ_{dc} and R_H . It is necessary to measure the conductivity limit σ_{∞} at high frequency²⁴ and the thermopower S , which both depend on n and p , in order to explain coherently the experimental data.

In Sec. II the general expressions of the transport coefficients in the presence of PF are derived. The experimental procedure is described in Sec. III. In Sec. IV, the experimental data obtained on a series of p - and n -type samples are reported and discussed.

II. EXPRESSIONS OF TRANSPORT COEFFICIENTS IN THE PRESENCE OF PF

The derivation of the expression of transport coefficients of inhomogeneous materials constitutes a very old problem. Rayleigh,²⁷ Lichtenecker,²⁸ and Landauer²⁹ proposed different laws in order to express the resistivity of binary systems or metallic mixtures, as a function of the concentrations and resistivities of the constituents. These derivations are based on different assumptions concerning

the spatial arrangement of the two species, or the neighborhood of the grains in the mixture. The validity of various models of conductivity in inhomogeneous systems has been extensively discussed particularly by Landauer,^{30(a)} Cohen *et al.*,^{30(b)} and Pike.^{30(c)} The situation is somewhat simpler in the case of a semiconductor nonuniformly doped because of the spatial continuity of the bands. The existence of long-range PF in insulators and compensated semiconductors was predicted independently by Wannier³¹ and by Shockley.¹⁸ Such fluctuations have later been considered by Keldysh and Proshko,¹⁹ Fritzsche,²⁰ and Schklowskii and Efros.³² These fluctuations are generally superposed to short-range fluctuations, mainly present in disordered glassy and amorphous semiconductors. Contrary to short-range fluctuations which fundamentally change the density of states, as shown by Anderson,³³ Mott,³⁴ and Cohen, Fritzsche, and Ovshinsky,³⁵ long-range PF leave the local band structure unchanged.¹⁹ We show below that, provided some general conditions on randomness and macroscopic homogeneity of the PF distribution are fulfilled, expressions of the transport coefficients at frequencies 0 and ∞ can be derived without referring to specific topological considerations. The expressions of the transport coefficients derived in previous papers^{22,24} must be generalized in order to take into account (i) the complete distribution function of PF, including wells and hills of maximum magnitude; (ii) the existence of both types of carriers.

A. Model

Let us first review the major features of the model of PF, which was proposed in previous papers,^{22–26} and discuss to what extent this model describes satisfactorily the physical situation in compensated semiconductors and in semi-insulating materials. The present paper concerns bulk materials, or films, grown in such experimental conditions that they are expected to be macroscopically homogeneous and isotropic; that means that the transport coefficients measured on any tiny measurable sample cut in the material are independent of the location and of the orientation of the sample. Long-range PF are produced by the nonuniform distribution of ionized impurities or defects randomly distributed in space, and therefore specific spatial arrangements such as heterostructures or superlattices are excluded in the present analysis. Due to the existence of PF, the material may be considered as a three-dimensional (3D) mosaic of domains, each one being characterized by a given value of the electrostatic potential, and therefore of the carrier density. We consider only long-range PF (i.e., the size of the domains is assumed larger than the mean free path) resulting likely from slow variations of the local thermodynamic or thermocinetic conditions during growth.^{23,25} On the other hand, the size of the domains is assumed much smaller than the size of any workable specimen, in agreement with various experimental observations^{36–40} so that any measurable sample consists of a random assembly of a large number of elementary domains with different carrier densities. Thus measurable transport coefficients are not local quantities, but average values over the sample. The

energy distribution of PF is assumed Gaussian, with a maximum probability at some energy E_{c0} for the conduction-band edge, and a standard deviation $\Gamma/\sqrt{2}$. In compensated materials PF are not appreciably screened by free carriers due to their very low total density. However the few existing electrons in the band accumulate at the bottom of the deepest wells, and the few holes at the top of the highest hills. This results in a local screening and a truncation of the Gaussian distribution at energies $E_{c0}-g_c\Gamma$ and $E_{c0}+g_v\Gamma$, where g_c and g_v are numbers generally smaller than 3. In the case of single-band conduction, in n -type materials for instance, the knowledge of the maximum height $g_v\Gamma$ of hills is unimportant because the electron density at $E_{c0}+g_v\Gamma$ is negligible when $g_v\Gamma/kT \gg 1$. So, in previous papers²²⁻²⁶ g_v was considered equal to g_c and this common value was called g . In the case of mixed conductivity, electrons accumulate in potential wells and holes in potential hills, so it is necessary to use in the calculation of the carrier densities the right values of both the maximum depth $g_c\Gamma$ of wells, and the maximum height $g_v\Gamma$ of hills. Since, in general, $n \neq p$, g_c and g_v are different and have different temperature dependences. In the chromium doped GaAs crystals considered in Sec. IV, and more generally in semi-insulating materials $g_c\Gamma < E_{c0}-E_F$ and $g_v\Gamma < E_F-E_{v0}$, so that the electron and hole populations are nondegenerate, even in wells and hills of maximum magnitude, and therefore classical statistics can be used. In high-quality crystals, energy-gap fluctuations are unlikely, so only covariant fluctuations of the band edges E_c, E_v are considered here: $E_c-E_v=E_G=\text{const}$ and also $E_{c0}-E_{v0}=E_G$. In the low-field stationary regime, the local majority carrier densities are not changed by the field, and no noticeable injection of minority carriers from p to n regions, or vice versa, can occur because the existence of continuous barriers across the sample is excluded in the case of randomly distributed PF. Therefore the local distribution of electrons and holes remains the same as in equilibrium, and the current through the sample is independent of recombination and diffusion processes. Electrons in the conduction band and holes in the valence band move independently and their local densities remain the same as in equilibrium. Moreover, tunneling of electrons through potential hills and of holes through potential wells is negligible because, in the case of long-range PF, the spatial extent of wells and hills is too large in order to allow noticeable tunneling.

In order to discuss dc transport, let us consider a plane (xOy) parallel to the applied dc field. The conduction-band-edge energy E_c varies from one point to another, and the surface $E_c(x,y)$ reflects the location and the magnitude of PF. This surface consists inevitably of a plateau corresponding to the most probable energy E_{c0} , with randomly distributed wells and hills.^{22,23} The probability $P(E_c-E_{c0})$ of these PF, and consequently their spatial extent, decrease rapidly as $|E_c-E_{c0}|$ increases. As a consequence of the assumption of macroscopic homogeneity, there are no potential barriers, channels, or filaments in the sample, so the regions corresponding to the wells ($E_c < E_{c0}$) cannot extend continuously to infinity. In order to move through the material, electrons of the

conduction band must have an energy equal or larger than the height of the barriers between separate wells. This limit is the energy E_{c0} of the plateau, which plays the role of a threshold or of a percolation energy. The probability of finding domains in which electrons of energy $E > E_{c0}$ exist increases rapidly with $E-E_{c0}$, so that these electrons are free to move continuously in a connex region extending to infinity, provided that they avoid the top of hills where $E_c > E$, like does the sea between islands. The mobility of these free electrons is only slightly reduced by the extra scattering by potential hills, which is low if the mean free path is smaller than the extent of PF. The average density n_f of electrons carrying dc current is directly related to the average current density through any physically attainable cross section of the sample: therefore n_f is equal to the average density of conduction-band electrons of energy larger than E_{c0} . When $g_c\Gamma/kT \gg 1$, n_f is much smaller than the total average electron density n in the band. As the frequency of the external field increases to infinity, the amplitude of the electron motion tends to zero, so that the high frequency limit $\sigma_{n\infty}$ of the conductivity is proportional to the total density n . Similarly, the threshold energy of holes carrying dc current is the most probable energy $E_{v0}=E_{c0}-E_G$ of the valence-band edge. The ratio p_f/p of the free to total hole densities is equal to n_f/n , in the absence of band-gap fluctuations, only if $g_v=g_c$.

In previous papers, two methods have been proposed in order to derive the dc conductivity expression. The first one,^{22,23} based on the consideration of the carrier densities n_f, p_f defined above, is unaware of the topological arrangement of wells and hills. In the second one,^{24,26} in order to get the expression of ac conductivity, a model of spatial arrangement of wells and hills was proposed, and a coefficient α , equal to the relative proportion of wells in the sample, was introduced in order to adjust the ac conductivity to the right value. The two methods lead to similar values and temperature dependences of the ratios n_f/n and p_f/p , with little relative discrepancy.²⁵ However, the absolute values found for n_f and p_f by the two methods can differ by a factor of few units. In the present paper, only transport coefficients measured in dc or very-high-frequency conditions are considered. So it is unnecessary to introduce topological assumptions, and in the following we refer it to be the basic model of Refs. 22 and 23. This model is generalized by taking into account the densities of band carriers in the potential wells and hills of maximum magnitude: the relative importance of these wells, compared to that of the Gaussian distribution of PF, increases rapidly as g_c and g_v become smaller than unity. The complete distribution function $P(E_c)$ consists therefore of a Gaussian truncated at $E_{c0}-g_c\Gamma$ and $E_{c0}+g_v\Gamma$, and of two δ functions representing the total probabilities $P(g_c)$ at $E_{c0}-g_c\Gamma$, and $P(g_v)$ at $E_{c0}+g_v\Gamma$. Introducing the reduced amplitude of the local potential fluctuation:

$$u = \left[\frac{E_c - E_{c0}}{\Gamma} \right] = \frac{\varepsilon_c}{\Gamma} \quad (1)$$

the expressions of $P(g_c)$ and $P(g_v)$ are

$$P(g_c) = \frac{1}{\sqrt{\pi}} \int_{g_c}^{\infty} \exp(-u^2) du, \quad (2)$$

$$P(g_v) = \frac{1}{\sqrt{\pi}} \int_{g_v}^{\infty} \exp(-u^2) du.$$

B. Conductivity

The total average carrier densities n, p , in the bands are related to the average densities N_{di}^+, N_{aj}^- of ionized donors and acceptors by the average neutrality equation:²²

$$n - p = \sum_i N_{di}^+ - \sum_j N_{aj}^-. \quad (3)$$

The calculation of the average densities N_{aj}^+, N_{aj}^- would require the knowledge of the local densities $N_{di}(u), N_{aj}(u)$, which are obviously unknown. It will be assumed, as in Refs. 22 and 24, that the distribution of deep centers is nearly uniform. Taking into account the total distribution function $P(E_c)$, the average ionization probability of deep donors becomes

$$N_{di}^+/N_{di} = \frac{1}{\sqrt{\pi}} \left[\int_{-g_c}^{g_v} \frac{\exp(-u^2) du}{1 + g_{di} \exp \left[\frac{E_F - E_{c0} + E_{di} - u \Gamma}{kT} \right]} + \frac{\int_{g_c}^{\infty} \exp(-u^2) du}{1 + g_{di} \exp \left[\frac{E_F - E_{c0} + E_{di} + g_c \Gamma}{kT} \right]} \right. \\ \left. + \frac{\int_{g_v}^{\infty} \exp(-u^2) du}{1 + g_{di} \exp \left[\frac{E_F - E_{c0} + E_{di} - g_v \Gamma}{kT} \right]} \right] \quad (4)$$

and a similar expression holds for N_{aj}^-/N_{aj} .

The high frequency limit σ_{∞} of the conductivity is the sum of the average conductivities $\sigma_{n\infty}$ and $\sigma_{p\infty}$ due to the entire populations of electrons and holes:

$$\sigma_{n\infty} = nq\mu_n, \quad \sigma_{p\infty} = pq\mu_p, \quad \sigma_{\infty} = \sigma_{n\infty} + \sigma_{p\infty}. \quad (5)$$

The contribution to $\sigma_{n\infty}$ of the electrons of energy comprised between E and $E + dE$, in a domain of band edge E_c , may be written as

$$d\sigma_{n\infty}(E, E_c) = A_n (E - E_c)^{\alpha_n + 3/2} \left[-\frac{\partial f}{\partial E} \right] dE, \quad (6)$$

where A_n is independent of E , and α_n is the exponent of the energy dependence of the relaxation time. Here we shall consider only nondegenerate semiconductors. The expression of $\sigma_{n\infty}$ can be obtained, in the following two ways.

(i) By summing $d\sigma_{n\infty}(E, E_c)$ weighted by the probability $P(E_c)$ over all values of $E_c \leq E$, and by introducing the variable $\varepsilon = E - E_{c0}$, we have

$$d\sigma_{n\infty}(\varepsilon) = \frac{A_n}{kT} \exp \left[\frac{E_F - E_{c0}}{kT} \right] \exp \left[-\frac{\varepsilon}{kT} \right] G_0(\varepsilon) d\varepsilon, \quad (7)$$

where

$$G_0(\varepsilon) = \frac{1}{\Gamma \sqrt{\pi}} \int_{-g_c \Gamma}^{\min(\varepsilon, g_v \Gamma)} (\varepsilon - \varepsilon_c)^{\alpha_n + 3/2} \exp \left[-\frac{\varepsilon_c^2}{\Gamma^2} \right] d\varepsilon_c \\ + (\varepsilon + g_c \Gamma)^{\alpha_n + 3/2} P(g_c) + (\varepsilon - g_v \Gamma)^{\alpha_n + 3/2} P(g_v). \quad (8)$$

Integrating over ε we obtain

$$\sigma_{n\infty} = \frac{A_n}{kT} \exp \left[\frac{E_F - E_{c0}}{kT} \right] \int_{-g_c \Gamma}^{\infty} \exp \left[-\frac{\varepsilon}{kT} \right] G_0(\varepsilon) d\varepsilon. \quad (9)$$

(ii) By summing first over E , the contribution of a domain of band-edge energy E_c is

$$d\sigma_{n\infty}(\varepsilon_c) = \frac{A_n}{kT} \exp \left[\frac{E_F - E_{c0}}{kT} \right] \exp \left[-\frac{\varepsilon_c}{kT} \right] \\ \times \int_{\varepsilon_c}^{\infty} (\varepsilon - \varepsilon_c)^{\alpha_n + 3/2} \exp \left[-\frac{\varepsilon - \varepsilon_c}{kT} \right] d\varepsilon \quad (10)$$

which, after integration, becomes

$$d\sigma_{n\infty}(\varepsilon_c) = \frac{A_n}{kT} [(\alpha_n + \frac{3}{2})!] (kT)^{\alpha_n + 5/2} \\ \times \exp \left[\frac{E_F - E_{c0}}{kT} \right] \exp \left[-\frac{\varepsilon_c}{kT} \right]. \quad (11)$$

The expression of $\sigma_{n\infty}$ is obtained by summing $P(\varepsilon_c) d\sigma_{n\infty}(\varepsilon_c)$:

$$\sigma_{n\infty} = \sigma_{n00} \left[\frac{1}{\Gamma \sqrt{\pi}} \int_{-g_c \Gamma}^{g_v \Gamma} \exp \left[-\frac{\varepsilon_c}{kT} - \frac{\varepsilon_c^2}{\Gamma^2} \right] d\varepsilon_c \right. \\ \left. + P(g_c) \exp \left[\frac{g_c \Gamma}{kT} \right] \right. \\ \left. + P(g_v) \exp \left[-\frac{g_v \Gamma}{kT} \right] \right], \quad (12)$$

where

$$\sigma_{n00} = \frac{A_n}{kT} [(\alpha_n + \frac{3}{2})!] (kT)^{\alpha_n + 5/2} \exp \left[\frac{E_F - E_{c0}}{kT} \right]. \quad (13)$$

In the absence of PF, i.e., when Γ tends to zero, the quantity between the brackets in Eq. (12) tends to unity. So σ_{n00} is the conductivity of a semiconductor free from PF:

$$\sigma_{n00} = q\mu_n N_c \exp \left[\frac{E_F - E_{c0}}{kT} \right]. \quad (14)$$

Equating the two expressions (9) and (12) of $\sigma_{n\infty}$, the following identity, which will be used below, is obtained:

$$\begin{aligned} \sigma'_{ndc} = \frac{A_n}{kT} \exp \left[\frac{E_F - E_{c0}}{kT} \right] & \left[\frac{1}{\Gamma\sqrt{\Pi}} \int_0^\infty \exp \left[-\frac{\epsilon}{kT} \right] \int_0^{\min\{\epsilon, g_v\Gamma\}} (\epsilon - \epsilon_c)^{\alpha_n + 3/2} \exp \left[-\frac{\epsilon_c^2}{\Gamma^2} \right] d\epsilon_c d\epsilon \right. \\ & \left. + P(g_v) \int_{g_v\Gamma}^\infty (\epsilon - g_v\Gamma)^{\alpha_n + 3/2} \exp \left[-\frac{\epsilon}{kT} \right] d\epsilon \right]. \quad (16) \end{aligned}$$

(ii) In the domains where $E_c < E_{c0}$, the free electrons are those with energy $E > E_{c0}$, and this corresponds to a conductivity

$$\begin{aligned} \sigma''_{ndc} = \frac{A_n}{kT} \exp \left[\frac{E_F - E_{c0}}{kT} \right] & \left[\frac{1}{\Gamma\sqrt{\Pi}} \int_0^\infty \exp \left[-\frac{\epsilon}{kT} \right] \int_{-g_c\Gamma}^{\min\{\epsilon, 0\}} (\epsilon - \epsilon_c)^{\alpha_n + 3/2} \exp \left[-\frac{\epsilon_c^2}{\Gamma^2} \right] d\epsilon_c d\epsilon \right. \\ & \left. + P(g_c) \int_0^\infty (\epsilon + g_c\Gamma)^{\alpha_n + 3/2} \exp \left[-\frac{\epsilon}{kT} \right] d\epsilon \right]. \quad (17) \end{aligned}$$

Therefore

$$\sigma_{ndc} = \sigma'_{ndc} + \sigma''_{ndc}. \quad (18)$$

Similar expressions are obtained for the dc conductivity σ_{pdc} of holes, by interchanging the suffixes n or c with p or v , and $E_F - E_{c0}$ by $E_{v0} - E_F$. Then the total dc conductivity in the mixed conduction regime is

$$\sigma_{dc} = \sigma_{ndc} + \sigma_{pdc}. \quad (19)$$

C. Hall coefficient

It is still assumed that PF are randomly distributed in space, and that their size is small enough so that an average conductivity of the material, independent of the size of the sample cross section and of its orientation, can be defined.

When R_H is measured with a dc current and a constant magnetic field, only the free carriers carry the current and are submitted to the Laplace force giving rise to the Hall voltage, so that the classical expression of R_H remains valid provided that the densities n_f and p_f of free carriers are used. The expression of the zero-field Hall coefficient measured under dc conditions is therefore

$$R_H = \frac{R_{nH}\sigma_{ndc}^2 + R_{pH}\sigma_{pdc}^2}{(\sigma_{ndc} + \sigma_{pdc})^2} = \frac{b_{dc}^2 R_{nH} + R_{pH}}{(b_{dc} + 1)^2} \quad (20)$$

$$\int_{-g_c\Gamma}^\infty \exp \left[-\frac{\epsilon}{kT} \right] G_0(\epsilon) d\epsilon = [(\alpha_n + \frac{3}{2})!] (kT)^{\alpha_n + 5/2} \sigma_{n\infty} / \sigma_{n00}. \quad (15)$$

When the sample is submitted to a dc field, the current is carried by free electrons of energy larger than E_{c0} . The dc conductivity σ_{ndc} is the sum of the following two terms. (i) In the domains where $E_c > E_{c0}$ all the electrons are free, so according to Eq. (7), the corresponding conductivity is equal to

with $R_{nH} = -r/n_f q$, $R_{pH} = r/p_f q$, and $b_{dc} = \sigma_{ndc}/\sigma_{pdc}$. The Hall coefficient remains negative as long as $p_f/n_f < (\mu_n/\mu_p)^2$. The Hall mobility, equal to

$$\mu_H = \left| \frac{-b_{dc}\mu_n + \mu_p}{b_{dc} + 1} \right| \quad (21)$$

reduces nearly to μ_n when n_f/p_f is large compared to $(\mu_p/\mu_n)^2$. Hall effect measurements can also be performed by using an ac current of angular frequency ω flowing through the sample. The conductivity is then a complex quantity²⁴ $\sigma_{ac}(\omega) + i\omega\epsilon_{ac}(\omega)$. The component of the Hall voltage in phase with the externally applied voltage is due to the Laplace force acting on the electron and holes carrying the in phase current. Therefore the real part of the Hall coefficient can be written as

$$R_H(\omega) = \frac{\mu_p\sigma_{pac}(\omega) - \mu_n\sigma_{nac}(\omega)}{[\sigma_{pac}(\omega) + \sigma_{nac}(\omega)]^2}, \quad (22)$$

where $\sigma_{pac}(\omega)$ and $\sigma_{nac}(\omega)$ are the real parts of the hole and electron conductivities.

D. Thermopower

Fritzsche⁴¹ derived, in the case of microscopically homogeneous semiconductors, a general expression for the thermopower without reference to a specific conduction

process. The thermopower is related to the Peltier coefficient Π by the classical relation

$$S = \frac{\Pi}{T}, \quad (23)$$

where Π is the energy relative to E_F carried by the electrons per unit charge. For electrons in the interval $(E, E + dE)$ the weighting factor⁴¹ is $\sigma(E)dE/\sigma$, where σ is the total conductivity

$$\sigma = \int \sigma(E)dE. \quad (24)$$

The expression of the thermopower derived by Fritzsche is thus

$$S = -\frac{k}{q} \int \left[\frac{E - E_F}{kT} \right] \frac{\sigma(E)}{\sigma} dE. \quad (25)$$

According to the definition of Π , the free energy of all the carriers of the bands must be taken into account. This remains true in the presence of PF, and is related to the fact that S is defined as the ratio of the variations of thermoelectric voltage and of temperature, at zero current. So, in a domain of band-edge energy E_c the contribution

to the conductivity of electrons in the energy range $(E, E + dE)$ is $d\sigma_{n\infty}(E, E_c) + d\sigma_{p\infty}(E, E_v)$ and the total conductivity σ at the denominator of the weighting factor is the total average conductivity of any workable sample, i.e., $\sigma_{\infty} = \sigma_{n\infty} + \sigma_{p\infty}$. Therefore,

$$dS(E, E_c) = -\frac{k}{q} \left[\frac{E - E_F}{kT} \right] \frac{d\sigma_{n\infty}(E, E_c) + d\sigma_{p\infty}(E, E_v)}{\sigma_{n\infty} + \sigma_{p\infty}}. \quad (26)$$

The total contribution of electrons of the interval $(E, E + dE)$ in all domains is obtained by summing the expression (26), weighted by the probability $P(E_c)$ or $P(E_v)$, over all the values of E_c or E_v . It is convenient to consider first the thermopower S_n which would result from the conduction-band electrons alone. From Eq. (26) we obtain

$$dS_n(\varepsilon) = -\frac{k}{q} \left[\frac{E_{c0} - E_F}{kT} + \frac{\varepsilon}{kT} \right] \frac{d\sigma_{n\infty}(\varepsilon)}{\sigma_{n\infty}}, \quad (27)$$

where $d\sigma_{n\infty}(\varepsilon)$ is given by Eq. (7). Then integrating over ε and using Eqs. (7) and (9) S_n is expressed as

$$S_n = -\frac{k}{q} \left[\frac{E_{c0} - E_F}{kT} + \frac{1}{kT} \int_{-g_c\Gamma}^{\infty} \varepsilon \exp(-\varepsilon/kT) G_0(\varepsilon) d\varepsilon / \int_{-g_c\Gamma}^{\infty} \exp(-\varepsilon/kT) G_0(\varepsilon) d\varepsilon \right]. \quad (28)$$

The numerator of the second term in parentheses is equal to the partial derivative, relative to $\beta = 1/kT$, of the denominator, with Γ , g_c , and g_v being kept constant. Using the identity (15), Eq. (28) finally takes the form

$$S_n = -\frac{k}{q} \left[\frac{E_{c0} - E_F}{kT} + \alpha_n + \frac{s}{2} - \beta \frac{\partial}{\partial \beta} \ln \left[\frac{\sigma_{n\infty}}{\sigma_{n00}} \right] \right]. \quad (29)$$

The quantity $U_n = \beta(\partial/\partial\beta)[\ln(\sigma_{n\infty}/\sigma_{n00})]$ which reflects the influence of PF on thermopower, is a function of Γ , g_c , and g_v ; from Eq. (12) we obtain

$$\begin{aligned} \frac{\partial}{\partial \beta} \left[\frac{\sigma_{n\infty}}{\sigma_{n00}} \right] &= \frac{\Gamma \exp \left[\frac{\beta^2 \Gamma^2}{4} \right]}{2\sqrt{\Pi}} \left\{ \beta \Gamma \int_{-g_c + \beta\Gamma/2}^{g_v + \beta\Gamma/2} \exp(-u^2) du + \exp \left[- \left[g_v + \frac{\beta\Gamma}{2} \right]^2 \right] - \exp \left[- \left[-g_c + \frac{\beta\Gamma}{2} \right]^2 \right] \right\} \\ &+ g_c \Gamma P(g_c) \exp(\beta g_c \Gamma) - g_v \Gamma P(g_v) \exp(-\beta g_v \Gamma). \end{aligned} \quad (30)$$

Therefore the general expression of U_n is easily calculated. Now, when g_c and g_v are large enough so that the terms containing $P(g_c)$ and $P(g_v)$ are negligible in Eqs. (12) and (30), U_n reduces to the simple expression

$$\beta \frac{\partial}{\partial \beta} \ln \left[\frac{\sigma_{n\infty}}{\sigma_{n00}} \right] = \frac{\beta^2 \Gamma^2}{2} - \frac{\beta \Gamma}{2} \frac{\exp[-(-g_c + \beta\Gamma/2)^2] - \exp[-(g_v + \beta\Gamma/2)^2]}{\int_{-g_c + \beta\Gamma/2}^{g_v + \beta\Gamma/2} \exp(-u^2) du}. \quad (31)$$

Similarly, we have for the valence band

$$S_p = \frac{k}{q} \left[\frac{E_F - E_{v0}}{kT} + \alpha_p + \frac{s}{2} - \beta \frac{\partial}{\partial \beta} \ln \left[\frac{\sigma_{p\infty}}{\sigma_{p00}} \right] \right]. \quad (32)$$

When both bands are populated, integration of Eq. (26)

leads to the following expression of the thermopower:

$$S = \frac{S_n \sigma_{n\infty} + S_p \sigma_{p\infty}}{\sigma_{n\infty} + \sigma_{p\infty}} \quad (33)$$

which shows that S depends on the average total densities of both types of carriers.

E. Possible situations in si-GaAs crystals

It results from the previous analysis that the transport coefficients of a semiconductor with potential fluctuations depend essentially on the respective values of the carrier densities n , p , n_f , and p_f . The following four different situations may therefore be encountered.

(i) $n > p$ and $n_f > p_f$: then $R_H < 0$, and it is easy to verify that also $S < 0$. This case corresponds, according to the usual criterions, to a purely n -type material even if at the top of some potential hills the local hole density may exceed the local electron density.

(ii) $n < p$ and $n_f > p_f$. Of course this situation could not be found in a material free from PF. But in a real crystal this case is not improbable, and may be found when g_c is sufficiently small compared to g_v : then most of the holes are in the potential hills while a significant proportion of the electrons are free. The Hall coefficient R_H is negative since $n_f > p_f$. The sign of the thermopower S [Eq. (33)] is negative if $|S_n|/S_p > \sigma_{p\infty}/\sigma_{n\infty}$, or positive if $|S_n|/S_p < \sigma_{p\infty}/\sigma_{n\infty}$. In the first case, the semiconductor is considered as n type; this situation is likely found in the data of Philadelphus and Euthymiou.⁴² In the second case, the semiconductor has a positive thermopower but a negative Hall coefficient. Most of the authors conclude that such samples with positive room temperature thermopower are p type. For this reason Look⁴³ has rejected possible solutions where $p_f < n_f$ because S was positive.

(iii) $n < p$ and $n_f < p_f$: except when $p_f/n_f > (\mu_n/\mu_p)^2$, $R_H < 0$, however as in (ii) S can be either positive or negative (Cronin and Haysty¹⁷). These samples are commonly considered as p type but, as shown in (ii), situations with $S > 0$ and $R_H < 0$ can also be found in " n -type" samples where $n_f > p_f$. Therefore if the existence of PF is neglected, the terms p - and n -type do not have a clear meaning.

(iv) $n > p$ and $n_f < p_f$. This situation is just the reverse of case (ii) and would happen when g_c is sufficiently larger than g_v . Such samples could hardly have a positive Hall coefficient, while the thermopower is negative. To our knowledge, this situation has never been experimentally met before in si-GaAs although this "anomaly" between the signs of R_H and S has been reported in the case of amorphous materials.^{44,45}

In summary, the necessary condition for mixed conductivity [cases (ii) and (iii)] is that the total hole density p exceeds the total electron density n , due to the large value of μ_n/μ_p . The most striking fact resulting from the existence of PF is that not only " p -type," but also " n -type" samples can exhibit mixed conduction. In order to determine the total carrier densities and the magnitude of PF, it is therefore necessary to measure at the same time σ_{dc} but also and especially S and σ_{∞} versus T , up to high temperature. The terms " p type," and " n type" are generally not well defined in the literature since three possible criteria can be chosen: the sign of thermopower, the sign of Hall coefficient, or the value of the ratio c of free carrier densities. In what follows, we shall adopt the third point of view. The material is said p type if, at least at room temperature, $p_f > n_f$, and it is said n type if $n_f > p_f$. Of course this classification is somewhat arbitrary since in

some cases a material can change from p to n type when the temperature varies.

III. EXPERIMENTAL PROCEDURE

All the samples considered in this work were cut, as parallelepipeds 0.3 mm thick, in chromium-doped si-GaAs single crystals. After chemically etching the surfaces, Ohmic contacts are made at the ends of the samples by evaporation of Au:Ge and annealing at 430°C in an Argon-Hydrogen atmosphere for one minute. During the measurements, which are performed in the temperature range extending from 300 to 450 K, the samples are maintained in vacuum, with a residual pressure lower than 10^{-5} Torr. For dc conductivity measurements, current is supplied by a Keithley 220 programmable current source, and the voltage is measured by a fully guarded digital electrometer Keithley 616, of input resistance larger than 10^{14} Ω , controlled by a microcomputer. The current versus voltage data are recorded in both current directions, at fields low enough to avoid field enhanced conductivity which has been observed in si-GaAs by Pistoulet and Abdalla.⁴⁶ In thermopower measurements, the temperature difference ΔT between the ends of the sample, is measured by a differential chromel-alumel thermocouple, and the emf ΔV across the sample is automatically plotted versus ΔT every 0.05 K. The thermoelectric power $S = d(\Delta V)/d(\Delta T)$ is calculated by a least-squares method. The sample is short circuited after each measurement. Before starting the cycle, each sample is preheated up to 420 K to insure equilibrium between centers and bands, and to eliminate possible surface films of water molecules.

The high-frequency measurements of σ_{∞} were performed in a coaxial line arranged in a special cryostat,²⁴ at frequencies larger than 10 MHz. The dc conductivity is also measured in this system, and the ratio $\sigma_{dc}/\sigma_{\infty}$ is determined at each temperature.

We have studied six samples, three " p type" and three " n type." The numbers by which the samples are designated, and their origins are as follows.

(i) " p type:" S-1 (Sumitomo); MR-22 (Metals research), and L-UA (LEP) unannealed.

(ii) " n type:" S-F2 (Sumitomo), RTC-UA (RTC) unannealed, and RTC-A (RTC) annealed.

Sample RTC-A was cut from the same crystal as sample RTC-UA, but was annealed at 900°C for 20 min.

IV. RESULTS AND DISCUSSION

Among the eight quantities Γ , g_c , g_v , $E_{c0} - E_F$, α_n , α_p , μ_n , and μ_p appearing in the four independent Eqs. (5), (9), (19), and (33), only the first four are really unknown. Above 300 K, phonon scattering is the most effective diffusion process, so both α_n and α_p can be considered equal to $-\frac{1}{2}$, and μ_n and μ_p proportional to $T^{-3/2}$, except when specifically mentioned. According to the data of the literature μ_n can be assumed equal to 4000 cm²/V s at

TABLE I. Characteristics of *p*-type samples at 298 and 420 K.

Sample	Γ (eV)	$\sigma_{dc}/\sigma_{\infty}$		$E_{c0}-E_F$ (eV)		Activation energy of σ_{dc} (eV)	
		298 K	420 K	298 K	420 K	298 K	420 K
MR-22	0.193	5.87×10^{-4}	0.250	0.769	0.712	0.530	0.820
S-1	0.193	6.67×10^{-4}	0.244	0.763	0.707	0.540	0.820
L-UA	0.198	4.11×10^{-4}	0.160	0.765	0.704	0.540	0.820

room temperature (except in sample S-F2 where the best fit is obtained with $\mu_n = 2600 \text{ cm}^2/\text{Vs}$) and the ratio μ_n/μ_p is assumed equal to 10. The uncertainty on the values of the mobilities is likely smaller than 50%, and the corresponding errors on the carrier densities do not affect appreciably the calculated Fermi energy. Numerical calculations have shown that changing the values of α_n , α_p , μ_n , and μ_p in reasonable limits does not change significantly the conclusions of our analysis.

The three quantities σ_{∞} , σ_{dc} , and S are measured versus temperature between 300 and 450 K. The unknown quantity Γ must be independent of temperature, and we have found that, for each sample, only a narrow range of Γ values allows a coherent fitting of the data. Once Γ is obtained, then the quantities g_c , g_v , $E_{c0}-E_F$, and E_F-E_{v0} which are determined by fitting σ_{dc} , σ_{∞} , and S are plotted versus temperature.

A. *p*-type samples

The experimental data for σ_{∞} , σ_{dc} , and S , concerning the three *p*-type samples are plotted versus $10^3/T$ in Figs. 1, 2, and 3. It is observed that the total conductivity σ_{∞} remains constant, roughly up to 400 K; this corresponds to the exhaustion of shallow and moderately deep centers. Above 400 K, the ionization of deep centers becomes predominant, and the total carrier density increases rapidly. The ratio $\sigma_{dc}/\sigma_{\infty}$, which is only of the order of 10^{-4}

at room temperature, increases with T , and would tend to unity only at very high temperature. Consequently, large errors could result if the carrier densities were deduced (as usually done in the literature) from σ_{dc} or R_H only. The magnitude of Γ calculated from σ_{∞} , σ_{dc} , and S , is of the order of 0.2 eV (Table I). This is larger than the values found in the case of crystals showing unipolar conduction.^{22,24} The slope of $\sigma_{dc}(1/T)$ is varying continuously and the flattening starts at relatively high temperature, below 400 K. This behavior has been previously reported,^{5,6} and was attributed to a surface conductance shunting the very high bulk resistance. However, this effect is often observed for different surface treatments, and with different geometrical configurations, so that it is doubtful that surface effects alone be responsible for this flattening. It has been shown in the case of conduction in a single band^{22,24} that in the presence of PF the "activation energy" of σ_{dc} decreases continuously from a value close to the ionization energy of deep centers at high temperature, to a very small value at low temperature. In the case of mixed conductivity, similar conclusions are reached by fitting the experimental data: the continuous flattening of the curves $\sigma_{dc}(1/T)$ at low temperature, which was unexplained in the literature, would result from the combined variations of $g_c\Gamma/kT$, $g_v\Gamma/kT$ (where g_c and g_v vary with T), and of $E_{c0}-E_F$. However, for the purpose of comparison with data from literature, the experimental values of activation energy of σ_{dc} at 298 and 420 K are listed in Table I. The Fermi level obtained from the fit-

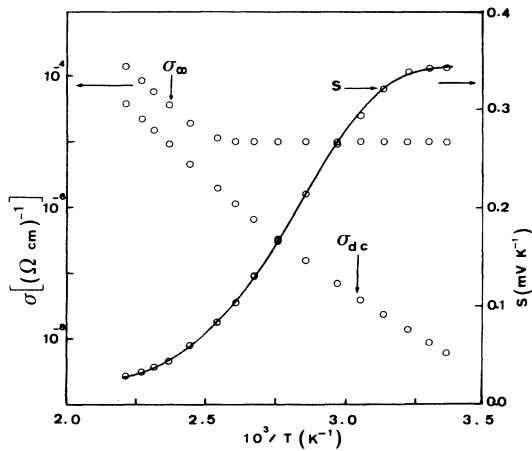


FIG. 1. *p*-type sample MR-22: (○) σ_{dc} , σ_{∞} , and S (experiment).

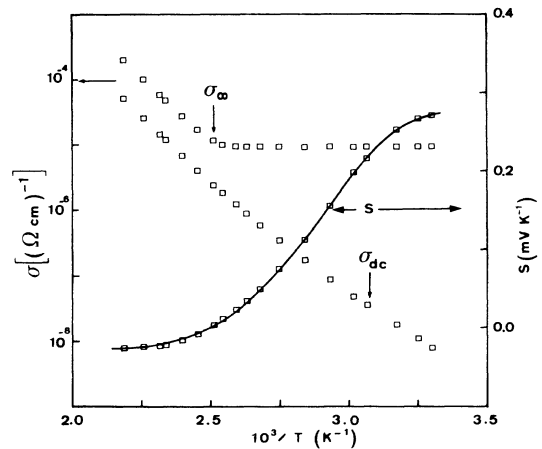


FIG. 2. *p*-type sample S-1: (□) σ_{dc} , σ_{∞} , and S (experiment).

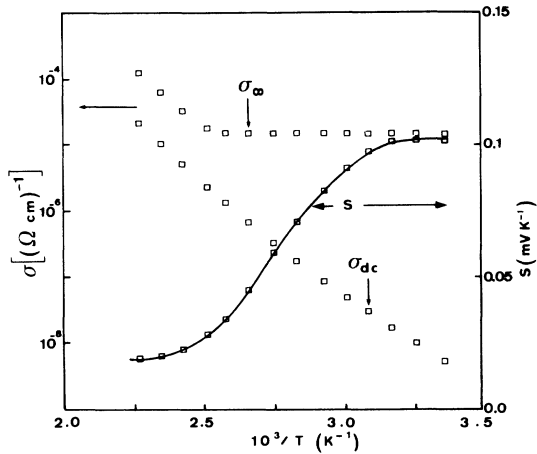


FIG. 3. *p*-type sample L-UA: (\square) σ_{dc} , σ_{∞} , and S (experiment).

ting is also indicated. We notice that it lies deep in the gap and is closer to the valence band than to the conduction band. The calculated values of $E_{c0} - E_F$, $E_{c0} - g_c \Gamma$, and $E_{c0} - E_G + g_v \Gamma$, are plotted versus T in Fig. 4 for sample MR-22. With regard to the low values of $E_F - E_{v0}$ it is clear that, in the absence of PF, these samples would be purely *p* type in contradiction with the mixed conduction behavior indicated by the experimental thermopower. At room temperature, the maximum depth $g_c \Gamma$ of the potential wells is larger than the height $g_v \Gamma$ of potential hills, but, as the temperature rises, g_c decreases from 2.9 to 1 and g_v from 1.35 to 0.29. According to Fig. 5, *p* is larger than *n* by a factor of 11 at room temperature, so holes accumulated at the top of the highest hills are screening more efficiently the hills than electrons are screening the potential wells. The decrease of g_c and g_v when T is raised results from the increase of the Debye length, and the ionization of deep centers and, when T increases, the Fermi level moves slightly in the gap. In spite

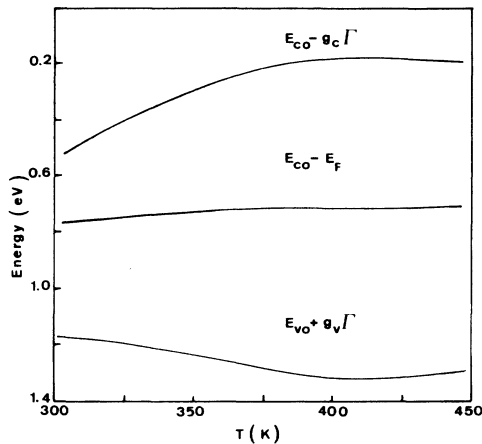


FIG. 4. (—) calculated values for MR-22.

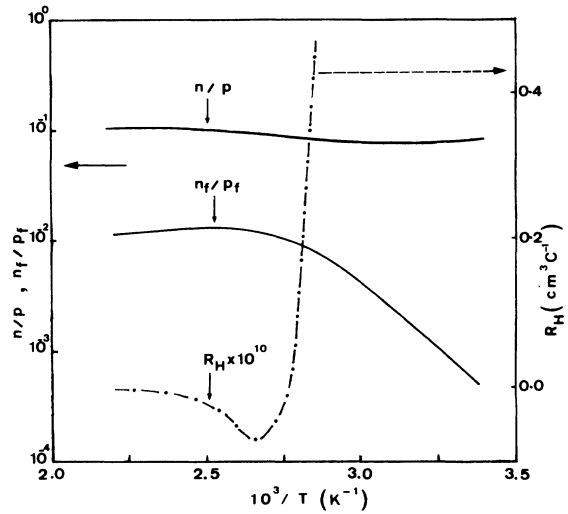


FIG. 5. Calculated n/p , n_f/p_f , and R_H for MR-22.

of its apparent complexity, the combined effect of the shift of the Fermi level and of the decrease of g_c and g_v can be simply represented by showing in Fig. 6, E_c , E_F , E_v , and the Cr energy level at two temperatures: 303 and 432 K. The abscissae represent the probability $P(E_c)$, and the average degree of ionization of the Cr centers can be easily deduced from the abscissa at which the energy line of the center crosses the Fermi level.

In Figs. 1, 2, and 3 we can easily observe that S remains positive in the whole temperature range for samples MR-22 and L-UA, while it becomes slightly negative above 400 K for sample S-1; this behavior explains why these samples are said *p* type. However the absolute value of S remains very low, and this can be explained only if the si-GaAs sample is in the mixed conductivity regime. On the other hand, the continuous variation of the slope of $S(T)$ cannot be accounted for in the case of unipolar conduc-

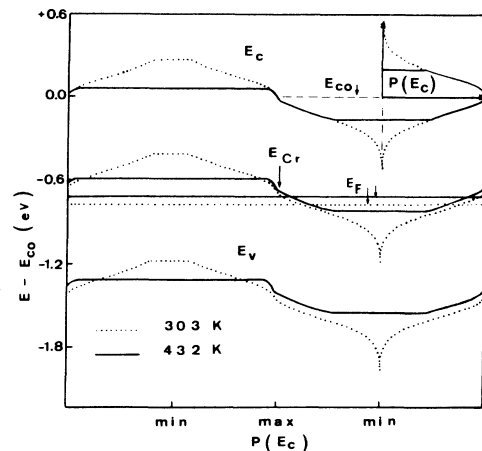


FIG. 6. Respective local positions of conduction and valence band edges, deep chromium, and Fermi levels for MR-22 at two temperatures.

TABLE II. Characteristics of *n*-type samples at 298 and 420 K.

Sample	Γ (eV)	$\sigma_{dc}/\sigma_{\infty}$		$E_{c0}-E_F$ (eV)		Activation energy of σ_{dc} (eV)	
		298 K	420 K	298 K	420 K	298 K	420 K
RTC-A	0.195	8.5×10^{-4}	0.230	0.631	0.626	0.592	0.730
RTC-UA	0.232	6.23×10^{-4}	0.410	0.632	0.618	0.600	0.775
S-F2	0.192	2.49×10^{-4}	0.272	0.651	0.638	0.545	0.815

tion. Therefore, there is no doubt on the existence of mixed conduction in the samples considered here. Furthermore, it must be noticed that it would be impossible to fit simultaneously $\sigma_{dc}(T)$ and $S(T)$ data if PF were disregarded. In order to study the behavior of the Hall coefficient $R_H(T)$ we have calculated its variations versus $10^3/T$. The R_H curves being similar for the three samples, we have plotted $R_H(1/T)$ for MR-22 in Fig. 5. It is interesting to notice that R_H is positive below room temperature, but becomes slightly negative above 360 K, where p_f/n_f is smaller [Eq. (20)] than $(\mu_n/\mu_p)^2 \simeq 10^2$, and where the ratio p/n does not vary significantly. A similar behavior for R_H was found by Look⁵ in some Cr-doped si-GaAs samples.

The "experimental intrinsic density" $n_{i\text{expt}}$ used in the literature is the square root of the product of the free carrier densities n_f and p_f . According to Eqs. (16) and (17), n_f is larger than $n_{00} = N_c \exp(E_F - E_{c0})/kT$ and p_f is larger than $p_{00} = N_v \exp(E_{v0} - E_F)/kT$ except for very small values of g_c and g_v . Therefore

$$n_{i\text{expt}} = (n_f p_f)^{1/2} > (n_{00} p_{00})^{1/2} = n_{i\text{theor}}. \quad (34)$$

At room temperature we find $n_{i\text{expt}} \simeq 1.3 n_{i\text{theor}}$ for the three *p*-type samples. As T is raised, Γ/kT decreases and therefore $n_{i\text{expt}}/n_{i\text{theor}}$ decreases also and tends to unity at very high temperature. This behavior of $n_{i\text{expt}}$ has been observed by many authors,^{7-9,13,16,43} but the origin of the discrepancy between $n_{i\text{expt}}$ and $n_{i\text{theor}}$ remained unsatisfactorily explained.

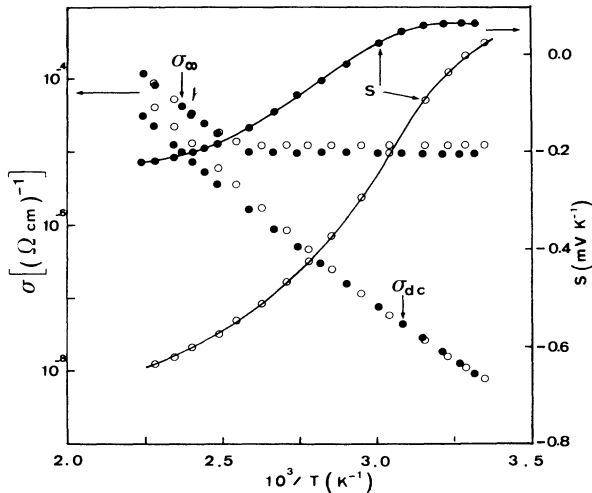


FIG. 7. *n*-type samples RTC: σ_{dc} , σ_{∞} , and S (experiment). (○) Unannealed; (●) annealed.

In summary, the three samples have nearly identical $\sigma_{dc}(1/T)$ characteristics, and in the absence of PF these samples should show similar values of the thermopower. This is not the case and, as it was indicated by the high value of the ratio $\sigma_{\infty}/\sigma_{dc}$, this is a new indication of the existence of PF.

B. *n*-type samples

σ_{dc} , σ_{∞} and S are plotted versus $(10^3/T)$ in Figs. 7 and 11, for three *n*-type samples. The thermopower is negative in the whole temperature range for sample S-F2, while it is positive below 340 K in sample RTC-A, and below 305 K in sample RTC-UA. S tends to saturate at low and high temperature, and the magnitude as well as the shape of $S(T)$ indicate that they result from mixed conduction. The procedure for determining the characteristics of the samples is the same as above except that for the samples RTC-UA and S-F2, temperature independent values of the mobilities were assumed in order to lead to a good fit. The values of Γ , of $E_{c0}-E_F$, and of the "activation energy" of σ_{dc} at 298 and 420 K are listed in Table II.

Let us examine first the samples RTC-UA and RTC-A. Figure 7 shows that σ_{∞} as well as σ_{dc} are slightly reduced by annealing but the reduction of $|S|$ is much more pronounced. In the two samples (Fig. 8), n_f is larger than p_f at all temperatures but the total density n is smaller than p . We observe that annealing produces an increase of the ratio p/n , and a decrease of Γ from 0.232 to 0.195 eV.

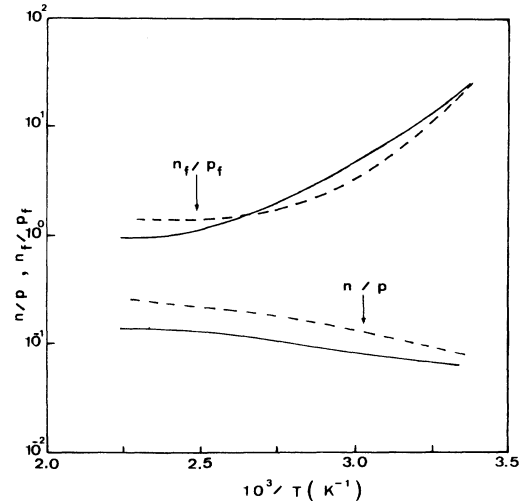


FIG. 8. Calculated n/p and n_f/p_f for samples RTC: (---) unannealed; (—) annealed.

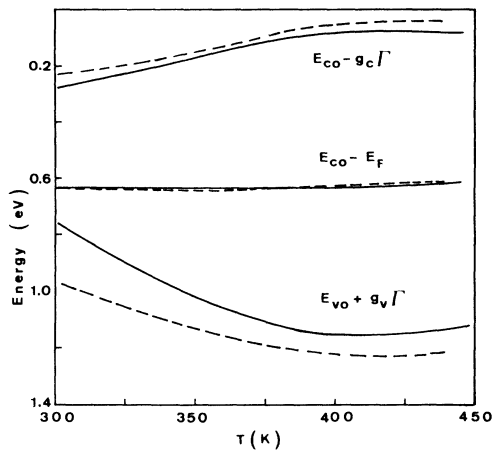


FIG. 9. Calculated values for samples RTC: (---) unannealed; (—) annealed.

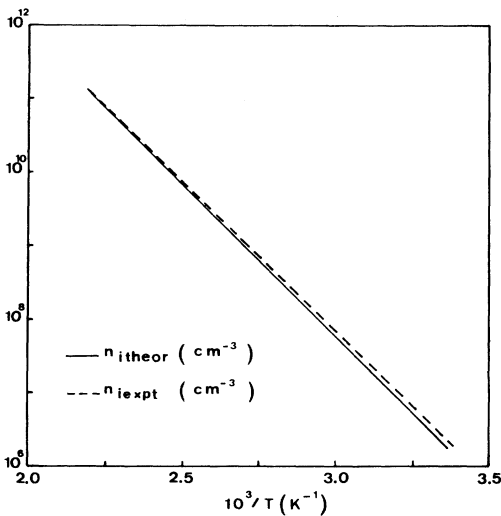


FIG. 10. Sample RTC-A: $n_{i th}$ and $n_{i expt} = (n_f/p_f)^{1/2}$.

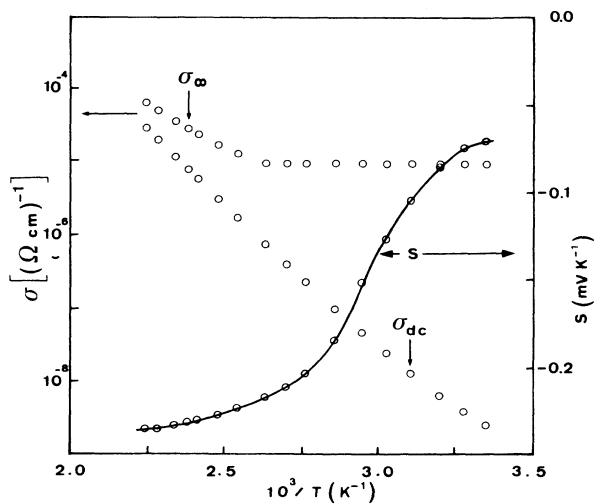


FIG. 11. *n*-type sample S-F2: (○) σ_{dc} , σ_{∞} , and *S* (experimental).

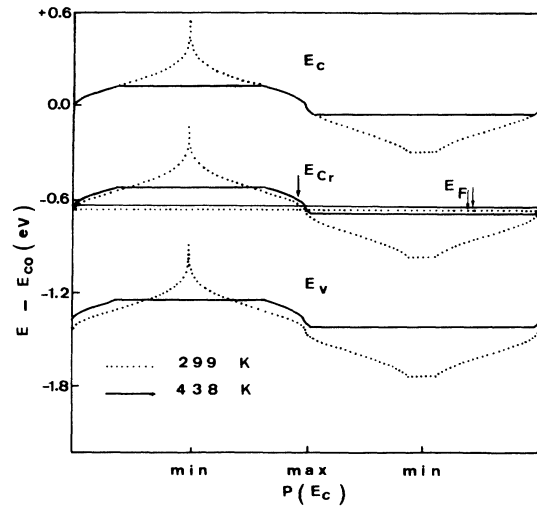


FIG. 12. Respective local positions of conduction- and valence-band edges, deep chromium, and Fermi levels for sample S-F2, at two temperatures.

The variations of the energies $E_{c0} - E_F$, and $E_{c0} - g_c \Gamma$ at the bottom of the wells, $E_{c0} - E_G + g_v \Gamma$ at the top of the hills are given in Fig. 9. Here, also, we observe that the Fermi level is close to the conduction band, so that a mixed conductivity would not be possible in the absence of PF. Moreover, although Γ is reduced by annealing, $g_c \Gamma$ and $g_v \Gamma$ are increased. We notice that in these *n*-type samples $g_v > g_c$, while for the *p*-type samples $g_c > g_v$. The experimental intrinsic density $n_{i expt}$ calculated for sample RTC-A is shown in Fig. 10. It remains always larger than the theoretical value to which it tends at high temperature for the reasons explained above.

For sample SF-2, the experimental curves $\sigma_{\infty}(1/T)$, $\sigma_{dc}(1/T)$ are similar to those of sample RTC-UA, but lower by a factor close to 1.8 for σ_{∞} and 2 for σ_{dc} , while the magnitude of *S* is smaller by a factor of 3 at high temperature (Fig. 11). The main difference is caused by a

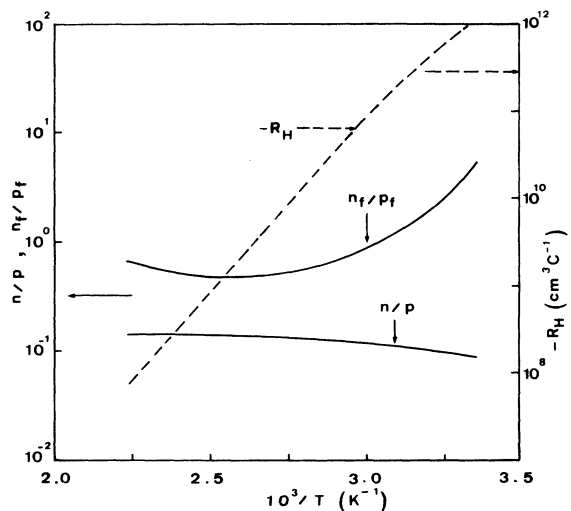


FIG. 13. Calculated n/p , n_f/p_f , and R_H for sample S-F2.

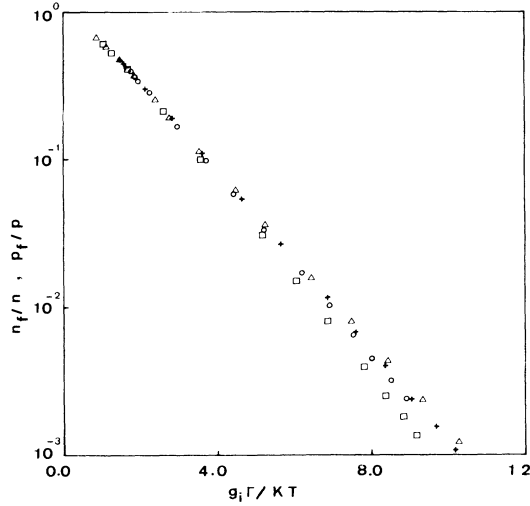


FIG. 14. n_f/n (n -type samples) and p_f/p (p -type samples) vs $g_c \Gamma / kT$ and $g_v \Gamma / kT$, respectively. (+) p type; (○) RTC-A; (△) SF-2; (□) RTC-UA.

larger value of g_c in sample SF-2. In this sample, $E_{c0} - E_F$ also remains nearly unchanged when T is raised and E_F crosses the Cr level near the maximum probability (Fig. 12). The Hall coefficient R_H calculated for this sample (Fig. 13) is nearly identical to that of a pure n -type sample because when $n_f \geq p_f$, the contribution of holes to R_H is negligible due to the large value of μ_n / μ_p . Thus it is clear that Hall effect measurements are inadequate for a complete analysis of the mixed conduction situation. The ratio n_f/n for the n -type samples and p_f/p for p -type samples is plotted versus $g_c \Gamma / kT$ and $g_v \Gamma / kT$, respectively, in Fig. 14. It is observed that this ratio varies exactly as $\exp(-(g_i \Gamma / \sqrt{2} kT))$ for p -type samples and for the RTC-A sample; it does not depart significantly from this law for the other samples. The quantity which reflects the fact that $p > n$ is the thermopower which remains pos-

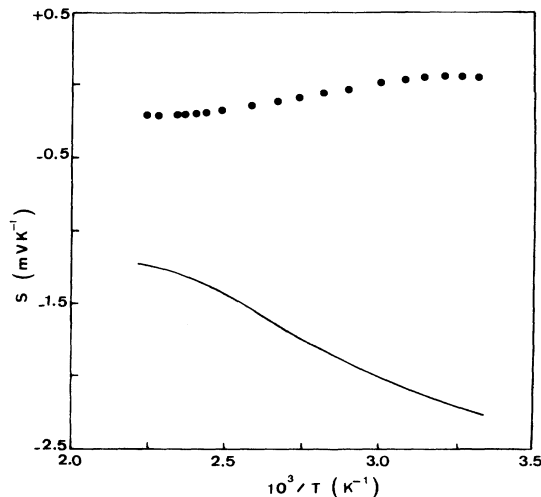


FIG. 15. Sample RTC-A: (●) S_{expt} ; (—) S' calculated if PF are neglected [Eq. (35)].

itive as long as $S_n \sigma_{n\infty} + S_p \sigma_{p\infty} > 0$, but, due to the temperature dependence of g_c and g_v , this inequality may be reversed. Thus a measurement of the sign of S by the hot probe method is quite insufficient in order to determine the type of the sample. As an illustration let us assume that the values of σ_{ndc} and σ_{pdc} are determined by galvanomagnetic measurements for sample RTC-A, and that E_F and the corresponding apparent thermopowers S_{ndc} and S_{pdc} are calculated from these values by neglecting in Eqs. (29) and (31) the terms corresponding to PF. We should obtain a total thermopower

$$S' = \frac{S_{ndc} \sigma_{ndc} + S_{pdc} \sigma_{pdc}}{\sigma_{ndc} + \sigma_{pdc}} \quad (35)$$

which is plotted in Fig. 15 together with the experimental data. The difference between the two behaviors is evident and consequently conclusive. Therefore, measurements of S , σ_{∞} , and σ_{dc} versus T above room temperature allow us to determine all the parameters which characterize the transport properties of the crystal.

V. CONCLUSION

The transport properties of si-GaAs:Cr are drastically changed by the existence of potential fluctuations which must necessarily be taken into account in order to obtain a coherent explanation of the experimental data in the case of mixed conduction. The dc conductivity, magnetoresistance, and Hall coefficient depend exclusively on the free carrier densities and do not give any information about the total carrier densities in the bands. We have systematically measured, for the first time, the thermoelectric power and the conductivity at high frequency in a large range of temperature above 300 K. These quantities which depend directly on the average total densities of electrons and holes allow us to determine the magnitude of the potential fluctuations, the Fermi energy, and the total carrier densities. It is found that in the six samples which were studied, Γ is of the order of 0.2 eV. On the other hand, the maximum magnitudes $g_c \Gamma$ and $g_v \Gamma$ of the fluctuations vary with T from about 0.2Γ to 3Γ depending on each case. Packets of electrons accumulate in deep wells and packets of holes in high hills, and this situation gives rise to a mixed conduction regime. It follows that the usual appellations of n and p type have no more a clear meaning and also that it is impossible to imagine a perfectly homogeneous semiconductor having the same transport coefficients as a microscopically disordered one. The reality is more subtle, especially in the case of mixed conduction.

By considering the existence of PF, the inconsistencies reported in the literature are removed. The disagreement between the sign of the Hall and the thermoprobe voltages, between the theoretical and "experimental" values of n_i , and also the reasons for the low values of the Fermi energies and the flattening of the $\sigma_{dc}(1/T)$ curves are easily explained. All the parameters Γ , g_c , g_v , n , and p should be taken into account, in order to get a realistic description of the properties of the semi-insulating materi-

al. This is the only way allowing reconciliation of experiment and theory. Moreover, our method can likely help to relate quantitatively the parameters responsible for the electronic properties to the changes in crystal-growth conditions and to the annealing processes.

ACKNOWLEDGMENT

The Laboratoire d'Automatique et de Microélectronique de Montpellier is "Laboratoire No. 371 associé au Centre National de la Recherche Scientifique."

- ¹D. C. Look, *J. Appl. Phys.* **48**, 5141 (1977).
- ²D. C. Look, *Solid State Commun.* **24**, 825 (1977).
- ³K. Kitahara, K. Nakai, A. Shibatomi, and S. Ohkawa, *Appl. Phys. Lett.* **32**, 259 (1978).
- ⁴A. L. Lin and R. H. Bube, *J. Appl. Phys.* **47**, 1859 (1976).
- ⁵D. C. Look, *J. Phys. Chem. Solids* **36**, 1311 (1975).
- ⁶T. Inoue and M. Ohyama, *Solid State Commun.* **8**, 1309 (1970).
- ⁷C. H. Gooch, C. Hilsum, and B. R. Holeman, *J. Appl. Phys.* **32**, 2069 (1961).
- ⁸R. H. Bube, *J. Appl. Phys.* **31**, 315 (1960).
- ⁹J. M. Whelan and G. H. Wheatley, *J. Phys. Chem. Solids* **6**, 169 (1958).
- ¹⁰J. S. Blakemore, *J. Appl. Phys.* **53**, R123 (1982).
- ¹¹D. D. Sell and H. C. Casey, *J. Appl. Phys.* **45**, 800 (1974).
- ¹²M. B. Panish and H. C. Casey, *J. Appl. Phys.* **40**, 163 (1969).
- ¹³J. Betko and K. Merinsky, *J. Appl. Phys.* **50**, 4212 (1979).
- ¹⁴J. Betko and K. Merinsky, *Phys. Status Solidi A* **77**, 331 (1983).
- ¹⁵L. Hrivnak, *Phys. Status Solidi A* **80**, 317 (1983).
- ¹⁶L. Hrivnak, *Phys. Status Solidi B* **127**, K165 (1985).
- ¹⁷G. R. Cronin and R. W. Haisty, *J. Electrochem. Soc.* **111**, 874 (1964).
- ¹⁸W. Shockley and J. Bardeen, *Phys. Rev.* **77**, 407 (1950).
- ¹⁹L. V. Keldysh and G. P. Proshko, *Fiz. Tverd. Tela (Leningrad)* **5**, 21 (1963) [*Sov. Phys.—Solid State* **5**, 13 (1964)].
- ²⁰H. Fritzsche, *J. Non-Cryst. Solids*, **6**, 49 (1971).
- ²¹B. I. Schklowskii and A. L. Efros, *Zh. Eksp. Teor. Fiz.* **60**, 867 (1971); **62**, 1156 (1972) [*Sov. Phys.—JETP* **33**, 468 (1971); **35**, 610 (1972)].
- ²²B. Pistoulet, P. Girard, and G. Hamamdjian, *J. Appl. Phys.* **56**, 2268 (1984); **56**, 2275 (1984).
- ²³B. Pistoulet, J. L. Robert, J. M. Dusseau, and L. Ensuque, *J. Non-Cryst. Solids* **29**, 29 (1978).
- ²⁴B. Pistoulet, F. M. Roche, and S. Abdalla, *Phys. Rev. B* **30**, 5987 (1984).
- ²⁵B. Pistoulet, P. Girard, and F. M. Roche, in *Physics of Disordered Materials*, edited by D. Adler, H. Fritzsche, and S. R. Ovshinsky (Plenum, New York, 1985), p. 425.
- ²⁶T. Soegandi, F. M. Roche, and B. Pistoulet, *Solid State Commun.* **55**, 967 (1985).
- ²⁷Lord Rayleigh, *Philos. Mag.* **34**, 481 (1892).
- ²⁸K. Lichtenecker, *Phys. Z.* **25**, 225 (1924).
- ²⁹R. Landauer, *J. Appl. Phys.* **23**, 779 (1952).
- ³⁰(a) R. Landauer, *Electrical Transport and Optical Properties of Inhomogeneous Media*, Proceedings of the First Conference on the Electrical Transport and Optical Properties in Inhomogeneous Media, AIP Conf. Proc. No. 80, edited by J. C. Garland and D. B. Tamer (AIP, New York, 1978), p. 2; (b) M. H. Cohen, J. Jortner, and I. Webman, *ibid.*, p. 63; (c) G. E. Pike, *ibid.*, p. 366.
- ³¹G. H. Wannier, *Phys. Rev.* **76**, 438 (1949).
- ³²B. I. Shklowskii and A. L. Efros, *Zh. Eksp. Teor. Fiz.* **61**, 816 (1971) [*Sov. Phys.—JETP* **34**, 435 (1972)]; *Fiz. Tekh. Poluprovodn.* **5**, 1938 (1971) [*Sov. Phys.—Semicond.* **5**, 1682 (1972)].
- ³³P. W. Anderson, *Phys. Rev. B* **5**, 2931 (1972).
- ³⁴N. F. Mott and E. A. Davis, *Electronic Processes in Non-Crystalline Materials* (Clarendon, Oxford, 1971); *Electronic Processes in Non-Crystalline Materials*, 2nd ed. (Oxford University Press, Oxford, 1979).
- ³⁵M. H. Cohen, H. Fritzsche, and S. R. Ovshinsky, *Phys. Rev. Lett.* **22**, 1065 (1969).
- ³⁶T. Matsuma, T. Obokata, and T. Fukuda, *J. Appl. Phys.* **57**, 1182 (1985).
- ³⁷D. Wruck, M. Seifert, and W. Ulrici, *Phys. Status Solidi A* **86**, 691 (1984).
- ³⁸J. C. Knights and R. A. Jujan, *Appl. Phys. Lett.* **35**, 244 (1979).
- ³⁹J. C. Knights, *J. Non-Cryst. Solids* **35& 36**, 159 (1980).
- ⁴⁰R. C. Ross, A. G. Johncock, and A. R. Chan, *J. Non-Cryst. Solids* **66**, 81 (1984).
- ⁴¹H. Fritzsche, *Solid State Commun.* **9**, 1813 (1971).
- ⁴²A. T. Philadelphus and P. C. Euthymiou, *J. Appl. Phys.* **51**, 2840 (1980).
- ⁴³D. C. Look, *Proceedings of the Conference on Semi-Insulating III-V Materials, Nottingham, 1980*, edited by G. J. Rees (Shiva Publ. Ltd., London, 1980), p. 183.
- ⁴⁴P. G. Le Comber, D. I. Jones, and W. E. Spear, *Philos. Mag.* **35**, 1173 (1977).
- ⁴⁵D. Emin, *Philos. Mag.* **35**, 1189 (1977).
- ⁴⁶B. Pistoulet and S. Abdalla, *J. Appl. Phys.* **60**, 1059 (1986).